Technical Report

Title: *Long-Term Strength Degradation Testing of DGR-3 and DGR-4 Core*

Document ID: TR-08-36

Authors: B. Gorski, T. Anderson and B. Conlon
CANMET Mining and Mineral Sciences Laboratories, Natural Resources Canada

Revision: 1

Date: June 18, 2010

DGR Site Characterization Document
Intera Engineering Project 08-200

| **Intera Engineering DGR Site Characterization Document** | | |
|---|---|---|
| Title: | Long-Term Strength Degradation Testing of DGR-3 and DGR-4 Core | |
| Document ID: | TR-08-36 | |
| Revision Number: | 1 | Date: June 18, 2010 |
| Authors: | B. Gorski, T. Anderson and B. Conlon, CANMET Mining and Mineral Sciences Laboratories | |
| Technical Review: | Kenneth Raven, Michael Melaney: Dougal McCreath (Laurentian University); Tom Lam, Jim McLay (NWMO) | |
| QA Review: | John Avis | |
| Approved by: | Kenneth Raven | |

| **Document Revision History** | | |
|---|---|---|
| Revision | Effective Date | Description of Changes |
| 0 | November 9, 2009 | Initial release |
| 1 | June 18, 2010 | Minor revisions to address NWMO editorial comments of June 15, 2010.<br><br>Updating of references. |
| | | |
| | | |
| | | |

# TABLE OF CONTENTS



## LIST OF APPENDICES

# 1 Introduction

Ontario Power Generation through the Nuclear Waste Management Organization (NWMO) is proposing to construct a Deep Geologic Repository (DGR) for low- and intermediate-level radioactive waste. The proposal calls for the DGR to be located at a depth of 680 m within the sedimentary bedrock beneath the Bruce Nuclear site near Tiverton, Ontario. NWMO has contracted Intera Engineering Ltd., Ottawa, Ontario to develop and implement a Geoscientific Site Characterisation Plan (GSCP) for the Bruce DGR. The GSCP is described by Intera Engineering Ltd. (2006, 2008a). The Bruce site overburden is underlain by near flat-lying Palaeozoic age dolostone, shale and limestone sedimentary rock to an estimated depth of approximately 860 m where Precambrian granite basement is encountered (Intera Engineering Ltd., 2009a).

Natural Resources Canada (NRCan) through the CANMET Mining and Mineral Sciences Laboratories (CANMET-MMSL) was contracted by Intera to provide laboratory geomechanical services. The objective of the current work to conduct mechanical tests on rock core samples originating from boreholes DGR-3 and DGR-4. Long-term Strength Degradation (LSD) and Uniaxial Compression Strength (UCS) tests comprised the bulk of the testing program. Supplemental acoustic emission (AE), velocity and post-failure testing were included in the program. This Technical Report (TR) describes the test apparatus and procedures and presents the results of the testing program.

Work described in this Technical Report was completed in accordance with Intera Test Plan TP-08-12 – Geomechanical Lab Testing of DGR-3 and DGR-4 Core (Intera Engineering Ltd., 2008b), prepared following the general requirements of the DGR Project Quality Plan (Intera Engineering Ltd., 2009b).

# 2 Standard Operating Procedures

The test program was carried out at the CANMET-MMSL's Rock Mechanics test facility located in Bells Corners, Ottawa. The Rock Mechanics test facility is managed by the Ground Control Program. The test facility is an ISO 17025 (International Standards Organization) accredited testing laboratory. Standard Operating Procedures (SOPs) that form part of the facility's accredited test procedures were selected for this project. The Standard Operating Procedures used for this test program were:

SOP-T 2100 Specimen Preparation, Standardization and Dimensional Tolerance Verification,

SOP-T 2103 Compressional P-Wave Velocity Test,

SOP-T 2112 Uniaxial Compressive Strength Test with Servo Computer Control Press, and

SOP-T 2113 Uniaxial Elastic Moduli and Poisson's Ratio Test with Servo Computer Control Press.

# 3 Specimens

Upon receipt the specimens were stored in an environmental chamber to minimize the loss or gain of moisture from the specimen. The 75-76 mm diameter specimens originated from boreholes DGR-3 and DGR-4. All samples submitted for testing were collected from the Cobourg Formation - Lower Member and were described as an argillaceous, mottled, slightly fossiliferous light/medium/dark grey limestone in this Technical Report. The total number of specimens received and tested comprised 6 long-term strength degradation tests (LSD) with 6 supplemental UCS tests.

The procedure for the preparation of a cylindrical specimen conforms to the ASTM standard, (ASTM D4543: 2008b) and CANMET-MMSL SOP-T 2100. The wet specimens were jacketed with heat-shrink tubing prior to sample preparation, to minimize the loss or gain of water. The end surfaces of specimens were ground flat to within 0.025 mm, parallel to each other to within 0.025 mm, and perpendicular to the longitudinal axis of the specimen to within 0.25 degrees as determined using a gauge plate and dial gauge.

Specimen lengths were determined to the nearest 0.025 mm by averaging the length measured at four points 90 degrees to each other. Specimen diameters were measured to the nearest 0.025 mm by averaging three measurements taken at the upper, middle and lower sections of the specimens. The average diameter was used for calculating the cross-sectional area. The volumes of the specimens were calculated from the average length and diameter measurements. The weights of the specimens were determined to the nearest 0.01 g and the densities of the specimens were computed to the nearest 0.001 Mg/m3. The borehole, depth, dimensions, bulk density, test type and geologic formation of each tested specimen, are listed in Table A-1. The measurements were repeated for LSD specimens prior to follow-up UCS tests.

Demec gauge reference disks were applied on the LSD test specimens for the measurement of deformations. Two axial demec gauges were bonded above and below the mid height of the specimen and in line with axis of the specimen with a gauge length of 95 mm. Similarly, two diametrically opposed circumferential demec gauges were mounted at 90 degrees to the axial gauges. The LSD wet specimens required that demec gauges be installed with applications of adhesive and a moisture barrier. A segment of the heat-shrink tubing was first removed from the gauge area. The rock surface was then dried, abraded, and the demec gauge was installed with an adhesive. A thick moisture protective coat was applied to the demec gauge and to the exposed specimen surfaces. Stainless steel platens were then installed on the specimen ends by wrapping the mating surfaces with moisture resistant tape.

# 4 Test Apparatus and Procedure

## 4.1 Zero Pressure Velocity Tests

Zero pressure P-wave and S-wave velocities were measured for all the UCS and LSD specimens prior to testing. The testing apparatus comprised a pulse generator, power amplifier, pulsing and sensing heads (transmitter and receiver) and oscilloscope. The P- and S-wave velocities were measured in accordance with SOP-T2103, and ASTM standard D 2845, (ASTM, 2008a).

## 4.2 Uniaxial Compression Strength Tests

Uniaxial compressive strength tests were conducted in a computer controlled, servo-hydraulic compression machine, consisting of a 2.22 MN rated load cell, load frame, hydraulic power supply, digital controller and test software. Three linear variable differential transformers (LVDTs) were arrayed around the specimen at 120 degree intervals for the measurement of axial deformations. A circumferential extensometer was used to measure specimen circumferential deformation.

The UCS test specimens were loaded in stress control to imminent failure at a rate of 0.75 MPa/s (ASTM D7012: 2007). The LSD UCS tests were loaded in circumferential displacement control through post-failure at a rate of 0.001 mm/s until residual stress was established. Data were scanned every second and stored digitally in engineering units. Time, axial load, axial strain and diametric strain were recorded during each test. The specimens were photographed before and after testing.

## 4.3 Acoustic Emission (AE) Tests

Acoustic emission tests were incorporated into the uniaxial compression tests. The AE system consisted of 12 transducer channels, 16 bit, 10 MHz, 40 dB preamplification, 60 dB gain, high and low pass filters and source location software.

Two outer arrays of 3 piezoelectric transducers each were attached to the surface of the uniaxial specimens. Arrays for uniaxial specimens were located in 1/3rd the length of the specimens. The transducers were spaced 120 degrees from each other for each array. The bottom array 1 consisted of transducers 1, 2 and 3 and the upper array 2 consisted of transducers 4, 5 and 6. The transducers were numbered clockwise looking down the specimen. Specimen references to top, bottom and down refer to the specimen orientation as retrieved from the borehole. Transducer 1 was orientated over the black line scribed on the specimen by Intera personnel. Transducer 4 on array 2 was rotated 60 degrees clockwise away from transducer 1 on array 1.

Acoustic emissions were recorded before, during and after each UCS test. Time, counts, magnitudes and other data were recorded for each event. The reader is referred to the research paper by Durrheim and Labrie (2007) where the acoustic system is explained in detail.

## 4.4 Long-Term Strength Degradation (LSD) Tests

The six LSD test specimens were installed in six hydraulic load frames. Two diametrically opposed AE sensors were installed at mid height on the surface of each test specimen. The AE sensors for all six specimens (12 sensors in total) were connected to the AE test system. The six specimens were loaded to stress values determined from the UCS test results. The specimen stress levels were monitored and held constant for 100 days. Acoustic emissions were recorded continuously during the tests. Time, counts, magnitudes and other data were also recorded for each event. AE data was downloaded weekly and reduced. Axial and diametric deformations were recorded weekly. Specimens were unloaded and removed after 100 days. The demec gauges and jacketing material were removed and the specimens were photographed. Dimensions, densities, P- and S-wave velocities and integrated post-failure AE-UCS tests were then performed on the specimens.

# 5 Analysis of Data

## 5.1 Zero Pressure Velocity Tests

The P- (compressive) and S-wave (shear) velocities were determined by dividing the specimen length by the wave travel time through the specimen. The dynamic properties were then calculated using the following equations:

Dynamic Young's Modulus

$$E_d = \frac{\rho V_s^2 \left(3V_p^2 - 4V_s^2\right)}{V_p^2 - V_s^2} \tag{1}$$

where: $E_d$ = dynamic Young's modulus
$V_s$ = shear wave velocity
$V_p$ = compressive wave velocity
$\rho$ = density

Dynamic Shear Modulus

$$G_d = \rho V_s^2 \tag{2}$$

where: $G_d$ = dynamic shear modulus
$V_s$ = shear wave velocity
$\rho$ = density

Poisson's Ratio (based on velocity data)

$$\nu_d = \frac{V_p^2 - 2V_s^2}{2\left(V_p^2 - V_s^2\right)} \tag{3}$$

where: $\nu_d$ = Poisson's Ratio
$V_s$ = shear wave velocity
$V_p$ = compressive wave velocity

The velocity measurements and calculated dynamic properties are contained in Table A-2. There were two sets of velocity measurements for each LSD test specimen. They were performed before and after the LSD test and prior to the subsequent UCS test.

## 5.2 Uniaxial Compression Strength Tests

Data obtained from the uniaxial compression tests included the axial stress (σ), the axial strain ($\varepsilon_a$) and the circumferential strain ($\varepsilon_c$). Strains were calculated using extensometer data. Stress and strain were calculated as follows:

Axial Stress

$$\sigma = \frac{P}{A_0} \tag{4}$$

where: $\sigma$ = axial stress
$P$ = applied axial load
$A_0$ = initial specimen cross-sectional area

Axial Strain

$$\varepsilon_a = \frac{\Delta l}{l_0} \tag{5}$$

where: $\varepsilon_a$ = axial strain
$\Delta l$ = change in length of specimen
$l_0$ = initial length of specimen

Circumferential Strain

$$\varepsilon_c = \frac{\Delta d}{d_0} \tag{6}$$

where: $\varepsilon_c$ = circumferential strain
$\Delta d$ = change in circumference of specimen
$d_0$ = initial circumference of specimen

Volumetric Strain

$$\varepsilon_v = \varepsilon_a + 2\varepsilon_c \tag{7}$$

where: $\varepsilon_v$ = volumetric strain
$\varepsilon_a$ = axial strain
$\varepsilon_c$ = circumferential strain

Ultimate uniaxial compressive strength $\sigma_c$, tangent Young's modulus of elasticity E, (calculated at 0.4 $\sigma_c$) and the Poisson's Ratio v, were established in each uniaxial test case as per (ASTM D7012: 2007) using load cell, extensometer and strain gauge data. These values were calculated as follows:

Ultimate Uniaxial Compressive Strength

$$\sigma_c = \frac{P_c}{A_0} \tag{8}$$

where: $\sigma_c$ = ultimate uniaxial compressive strength
$P$ = axial load at failure
$A_0$ = initial specimen cross-sectional area

Young's Modulus of Elasticity

$$E = \frac{\sigma_{40}}{\varepsilon_{40}} \tag{9}$$

where: $E$ = tangent Young's Modulus at 40% of peak strength
$\sigma_{40}$ = tangent stress at 40% of peak strength
$\varepsilon_{40}$ = tangent strain at 40% of peak strength

Poisson's Ratio

$$\nu = \frac{E_{axial}}{E_{lateral}} \tag{10}$$

where: $\nu$ = Poisson's Ratio
$E_{axial}$ = slope of axial stress-strain curve at 40% of peak strength
$E_{lateral}$ = slope of lateral stress-strain curve at 40% of peak strength

The ultimate uniaxial compressive strength, peak strain, Young's Modulus and Poisson's Ratio values are contained in Table A-3. Specimen stress-strain curves are contained in Appendix B. The graphs display stress-strain data calculated using extensometers.

Crack damage stress $\sigma_{cd}$, is the stress level where the $\varepsilon_v$-$\varepsilon_a$ curve reaches a maximum and starts to reverse in direction, indicating dilation due to the formation and growth of unstable cracks. Progressive fracturing failure process starts above $\sigma_{cd}$ leading to the failure of the rock. Crack damage stress and crack initiation stress levels are contained in Table A-3. Volumetric strain and crack volumetric strain curves are displayed in Appendix B. Appendix C contains photographs of the failed specimens.

Crack initiation stress $\sigma_{ci}$, is the stress level where the $\sigma$-$\varepsilon_a$ and $\varepsilon_{dv}$-$\varepsilon_a$ curves start to deviate from linear elastic behaviour, indicating the development and growth of stable cracks. The crack volumetric strain $\varepsilon_{dv}$ is the difference between the volumetric strain $\varepsilon_v$ observed in the test and the elastic volumetric strain $\varepsilon_{ev}$ calculated by assuming ideal linear elastic behaviour throughout the test. The value of $\sigma_{ci}$, was derived from the plot of the $\varepsilon_{dv}$-$\varepsilon_a$ curve.

Crack Volumetric Strain

$$\varepsilon_{dv} = \varepsilon_v - \varepsilon_{ev} \tag{11}$$

## 5.3 Acoustic Emission (AE) Tests

Acoustic Emission (AE) tests provided a non-destructive analysis of micro-crack formation, orientations and mechanisms and their effect on the mechanics of a test specimen. Coalescence of micro-cracks into macro-cracks cause major damage to a specimen and eventually leads to failure. AE are sound waves emitted by micro-cracks as they are created or move. Sound waves propagated through the specimen and were recorded continuously during the uniaxial compressive test.

Cumulative counts were recorded from the 6 AE channels during uniaxial compression testing. AE counts showed the amount of fracturing that occurred in the specimen. The cumulative hits for the six channels were summed and are plotted as hits versus in Appendix B and hits versus time in Appendix E. The source locations of AE events are shown displayed three-dimensionally (3D), adjacent to the photograph of the actual failed specimen in Appendices C. The 3D graph and the photograph are displayed vertically as per the test configuration. AE transducer locations are shown in green and the source locations are shown in red. AE source locations delineated regions of damage. Micro-crack distributions, mapped in 3D through time, describe damage accumulation, crack coalescence and macro-fracture propagation.

## 5.4 Long-Term Strength Degradation (LSD) Tests

The LSD tests were completed in April of 2009. The specimen LSD stress levels used during the experiments are shown in Table A-3. Axial and diametric deformations were recorded weekly. The diametric and axial strain measurements versus time are shown graphically for each specimen in Appendix D. AE data were downloaded weekly, reduced and compiled for the 100 day test duration. Cumulative AE hits versus time data for all six specimens are displayed graphically in Appendix E.

# 6 Results and Conclusions

This report has described the apparatus and procedures used to conduct various mechanical and dynamic property tests on rock units originating from sedimentary bedrock underlying the Bruce site. In accordance with ASTM guide D5878 (ASTM 2008c), the UCS tests indicate that the Cobourg Formation - Lower Member is in the category of, strong - very strong, with a 50-250 MPa strength range.

Young's modulus and Poisson's ratio values were consistent with the strength determinations. Inspection of stress-strain curves contained in Appendix B, Figures B-13 to B-16, indicate post-failure residual stress levels to be less than the recorded crack initiation stress levels. AE curves of cumulative hits increase and coincide with the stress-strain curve shifts contained in Appendix B.

Measurements taken before and after LSD tests indicate specimens shortened, the diameters increased, P and S-wave velocities increased and the dynamic modulus increased. Major trends were not evident between the static elastic constants of UCS and LSD sets of specimens. The majority of AE hits occurred during the first 60 days of the LSD tests.

# 7 Data Quality and Use

Data on geomechanical strength properties of DGR-3 and DGR-4 core described in this Technical Report are based on testing conducted in accordance with established and well defined ASTM testing procedures.

The results presented in this Technical Report are suitable for assessing the geomechanical strength properties of bedrock formations intersected by DGR-3 and DGR-4, and the development of descriptive geomechanical models of the Bruce DGR site

# 8 References

ASTM, 2008a. Designation D2845: Standard Test Method for Laboratory Determination of Pulse Velocities and Ultrasonic Constants of Rock, 2008 Annual Book of ASTM Standards, Section 4: Construction, Volume 04.08: Soil and Rock (I), ASTM International, West Conshohocken (PA), pp. 303-308.

ASTM, 2008b. Designation D4543: Standard Practices for Preparing Rock Core as Cylindrical Test Specimens and Verifying Conformance to Dimensional and Shape Tolerances, 2008 Annual Book of ASTM Standards, Section 4: Construction, Volume 04.08: Soil and Rock (I), ASTM International, West Conshohocken (PA), pp. 725-730.

ASTM, 2008c. Designation D5878: Standard Guides for Using Rock-Mass Classification Systems for Engineering Purposes, 2007 Annual Book of ASTM Standards, Section 4: Construction, Volume 04.09: Soil and Rock (II), ASTM International, West Conshohocken (PA), pp. 330-359.

ASTM, 2007. Designation D7012: Standard Test Method for Compressive Strength and Elastic Moduli of Intact Rock Core Specimens under Varying States of Stress and Temperatures; 2007 Annual Book of ASTM Standards, Section 4: Construction, Volume 04.09: Soil and Rock (II), ASTM International, West Conshohocken (PA), pp. 1429-1436.

Durrheim, R.J. and D. Labrie, 2007. Data-Driven Simulation of the Rock Mass response to Mining (Part 1): Laboratory Experimentation using Nepean Sandstone Models, In: Challenges in Deep and High Stress Mining, Y. Potvin, J. Hadjigeorgiou and D. Stacey, Editors, Australian Centre for Geomechanics (ACG), Chapter 34, pp. 293-304.

Intera Engineering Ltd., 2009a. Technical Report: Bedrock Formations in DGR-1, DGR-2, DGR-3 and DGR-4, TR-08-12, Revision 1, March 25, Ottawa.

Intera Engineering Ltd., 2009b. Project Quality Plan, DGR Site Characterization, Revision 4, August 14, Ottawa.

Intera Engineering Ltd., 2008a. Phase 2 Geoscientific Site Characterization Plan, OPG's Deep Geologic Repository for Low and Intermediate Level Waste, Report INTERA 06-219.50-Phase 2 GSCP-R0, OPG 00216-REP-03902-00006-R00, April, Ottawa.

Intera Engineering Ltd., 2008b. Test Plan for Geomechanical Lab Testing of DGR-3 and DGR-4 Core, TP-08-12, Revision 1, July 25, Ottawa.

Intera Engineering Ltd., 2006. Geoscientific Site Characterization Plan, OPG's Deep Geologic Repository for Low and Intermediate Level Waste, Report INTERA 05-220-1, OPG 00216-REP-03902-00002-R00, April, Ottawa.

# APPENDIX A

***Data and Calculation Tables***

Table A-1 Formations, Dimensions and Densities of Specimens

| Formation | Depth | Length | Diameter | Mass | Density |
|---|---|---|---|---|---|
| | (m) | (mm) | (mm) | (g) | (g/cm³) |
| DGR-3 | | | | | |
| Cobourg-Lower Member | 676.42 | 170.92 | 75.05 | 2013.77 | 2.66 |
| Cobourg-Lower Member | 676.67<br>(After LSD) | 170.79<br>(170.55) | 74.89<br>(75.20) | 2036.25<br>(2033.87) | 2.71<br>(2.69) |
| Cobourg-Lower Member | 680.21 | 170.68 | 75.45 | 2043.72 | 2.68 |
| Cobourg-Lower Member | 681.76<br>(After LSD) | 171.37<br>(171.01) | 75.47<br>(75.61) | 2052.32<br>(2050.75) | 2.68<br>(2.67) |
| Cobourg-Lower Member | 688.13 | 151.82 | 75.63 | 1806.34 | 2.65 |
| Cobourg-Lower Member | 688.28<br>(After LSD) | 146.60<br>(146.07) | 75.63<br>(75.45) | 1745.14<br>(1756.65) | 2.65<br>(2.69) |
| DGR-4 | | | | | |
| Cobourg-Lower Member | 664.46 | 171.07 | 75.62 | 2061.13 | 2.68 |
| Cobourg-Lower Member | 664.66<br>(After LSD) | 170.76<br>(170.67) | 75.64<br>(75.66) | 2054.46<br>(2056.02) | 2.68<br>(2.68) |
| Cobourg-Lower Member | 669.90 | 170.47 | 75.68 | 2060.61 | 2.69 |
| Cobourg-Lower Member | 670.10<br>(After LSD) | 171.25<br>(171.19) | 75.71<br>(75.72) | 2069.75<br>(2071.48) | 2.68<br>(2.69) |
| Cobourg-Lower Member | 674.16 | 171.89 | 75.66 | 2065.38 | 2.67 |
| Cobourg-Lower Member | 674.34<br>(After LSD) | 170.39<br>(170.48) | 75.58<br>(75.70) | 2048.90<br>(2050.84) | 2.68<br>(2.67) |

Table A-2 Dynamic Elastic Constants of Specimens

| Test Type | Depth | Length | P-wave time | P-wave velocity | S-wave time | S-wave velocity | E | Shear modulus | Poisson's ratio |
|---|---|---|---|---|---|---|---|---|---|
| | (m) | (mm) | (μs) | (km/s) | (μs) | (km/s) | (GPa) | (GPa) | ($\nu_d$) |
| DGR-3 | | | | | | | | | |
| UCS | 676.42 | 170.92 | 36.4 | 4.70 | 66.0 | 2.59 | 45.78 | 17.88 | 0.28 |
| Before LSD | 676.67 | 170.79 | 31.6 | 5.40 | 58.2 | 2.93 | 60.18 | 23.31 | 0.29 |
| After LSD | | 170.55 | 30.8 | 5.54 | 55.6 | 3.07 | 64.61 | 25.27 | 0.28 |
| UCS | 680.21 | 170.68 | 33.2 | 5.14 | 57.2 | 2.98 | 59.43 | 23.85 | 0.25 |
| Before LSD | 681.76 | 171.37 | 34.8 | 4.92 | 61.6 | 2.78 | 52.44 | 20.72 | 0.27 |
| After LSD | | 171.01 | 32.0 | 5.34 | 57.2 | 2.99 | 60.74 | 23.87 | 0.27 |
| UCS | 688.13 | 151.82 | 31.6 | 4.80 | 55.6 | 2.73 | 49.81 | 19.75 | 0.26 |
| Before LSD | 688.28 | 146.60 | 29.6 | 4.95 | 52.0 | 2.82 | 53.08 | 21.06 | 0.26 |
| After LSD | | 146.07 | 27.6 | 5.29 | 53.2 | 2.75 | 53.36 | 20.28 | 0.32 |
| DGR-4 | | | | | | | | | |
| UCS | 664.46 | 171.07 | 31.6 | 5.41 | 57.6 | 2.97 | 60.80 | 23.66 | 0.28 |
| Before LSD | 664.66 | 170.76 | 30.8 | 5.54 | 58.0 | 2.94 | 60.51 | 23.21 | 0.30 |
| After LSD | | 170.67 | 31.0 | 5.51 | 57.0 | 2.99 | 61.98 | 24.02 | 0.29 |
| UCS | 669.90 | 170.47 | 30.8 | 5.53 | 56.6 | 3.01 | 62.87 | 24.38 | 0.29 |
| Before LSD | 670.10 | 171.25 | 30.4 | 5.63 | 56.0 | 3.06 | 64.83 | 25.11 | 0.29 |
| After LSD | | 171.19 | 30.4 | 5.63 | 54.8 | 3.12 | 67.01 | 26.22 | 0.28 |
| UCS | 674.16 | 171.89 | 32.4 | 5.31 | 58.6 | 2.93 | 58.87 | 23.00 | 0.28 |
| Before LSD | 674.34 | 170.39 | 32.8 | 5.19 | 59.0 | 2.89 | 57.07 | 22.36 | 0.28 |
| After LSD | | 170.48 | 30.8 | 5.54 | 56.0 | 3.04 | 63.57 | 24.77 | 0.28 |

Table A-3 Static Elastic Constants of Specimens

| Test Type | Depth | LSD stress level | Ultimate uniaxial strength | Transducers | | | | | |
|---|---|---|---|---|---|---|---|---|---|
| | | | | Peak strain | E | Poisson's ratio | Crack damage stress | Crack Initiation stress | Post-Failure residual stress |
| | (m) | (MPa) | (MPa) | (%) | (GPa) | ($\nu$) | ($\sigma_{cd}$ =MPa) | ($\sigma_{ci}$ =MPa) | ($\sigma_r$ =MPa) |
| DGR-3 | | | | | | | | | |
| UCS | 676.42 | n/a | 75.22 | 0.37 | 28.41 | 0.22 | n/a | 30.30 | |
| LSD | 676.67 | 26 | 113.50 | 0.27 | 47.51 | 0.22 | 113.50 | 45.97 | 44.16 |
| UCS | 680.21 | n/a | 115.25 | 0.33 | 39.86 | 0.33 | 108.14 | 45.40 | |
| LSD | 681.76 | 40 | 103.22 | 0.28 | 34.24 | 0.22 | 103.22 | 42.10 | failed at peak |
| UCS | 688.13 | n/a | 76.09 | 0.36 | 21.35 | 0.35 | 64.05 | 29.84 | |
| LSD | 688.28 | 27 | 109.54 | 0.32 | 40.21 | 0.25 | 108.96 | 40.94 | 19.01 |
| DGR-4 | | | | | | | | | |
| UCS | 664.46 | n/a | 134.67 | 0.44 | 35.39 | 0.41 | 112.31 | 51.53 | |
| LSD | 664.66 | 47 | 90.26 | 0.26 | 36.59 | 0.21 | 87.45 | 37.76 | failed at peak |
| UCS | 669.90 | n/a | 88.69 | 0.25 | 40.63 | 0.32 | 83.60 | 36.34 | |
| LSD | 670.10 | 31 | 127.92 | 0.29 | 50.52 | 0.28 | 114.95 | 50.63 | 15.22 |
| UCS | 674.16 | n/a | 116.25 | 0.39 | 34.47 | 0.41 | 85.49 | 44.75 | |
| LSD | 674.34 | 41 | 96.68 | 0.21 | 42.76 | 0.24 | 93.26 | 37.91 | 11.88 |

# APPENDIX B

## *Stress-Strain Curves*

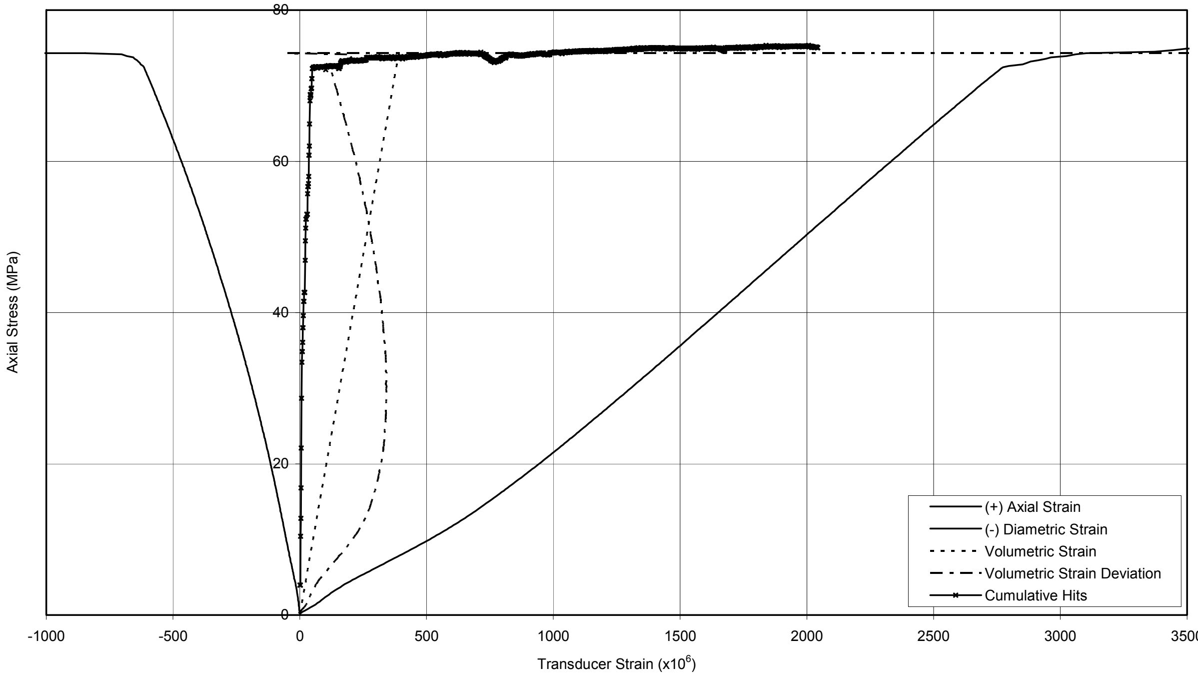


Figure B-1 UCS Specimen DGR-3, 676.42 m

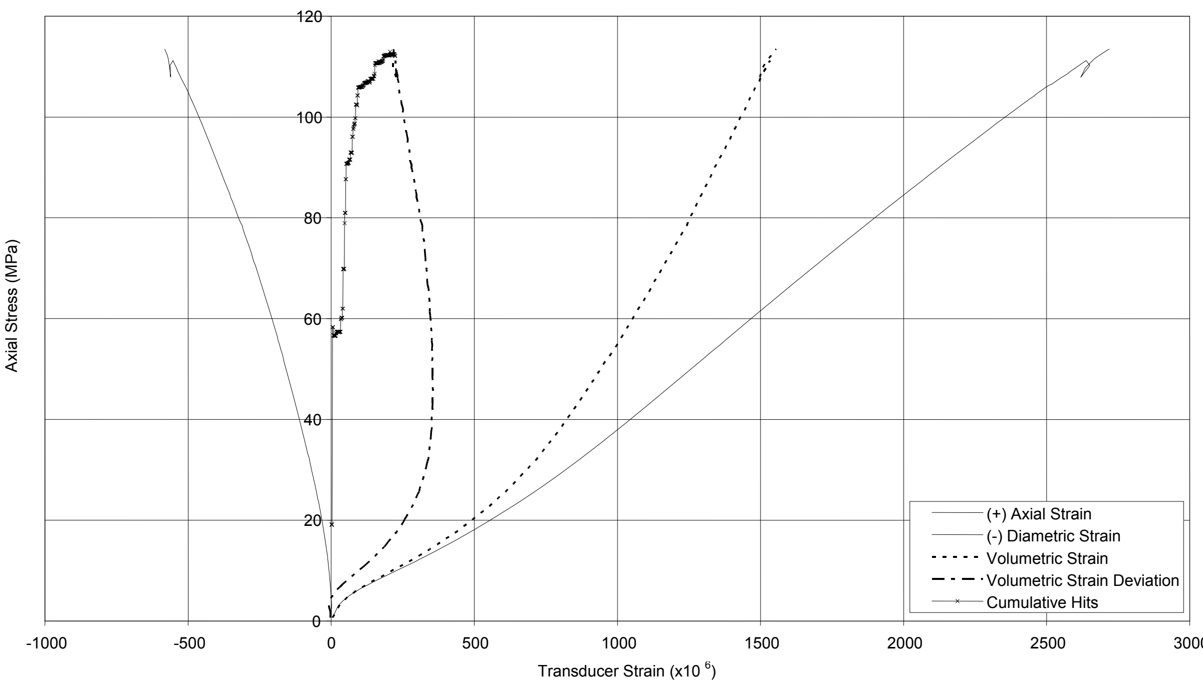


Figure B-2 UCS LSD Specimen DGR-3, 676.67 m

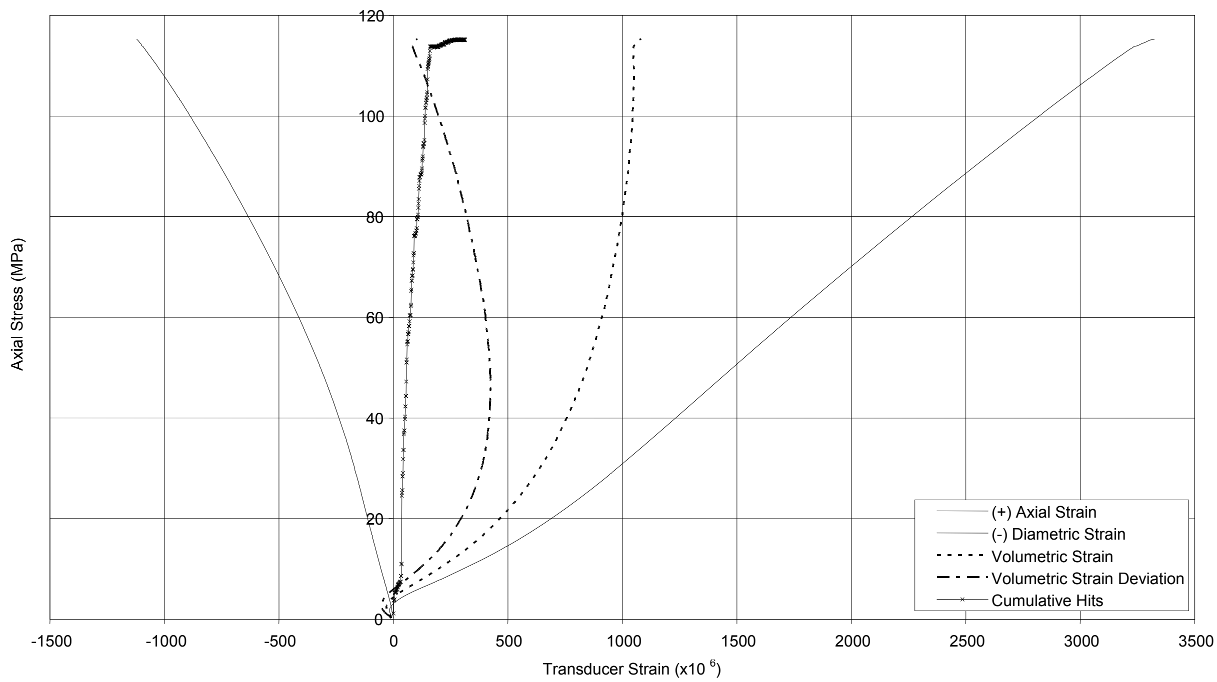


Figure B-3 UCS Specimen DGR-3, 680.21 m

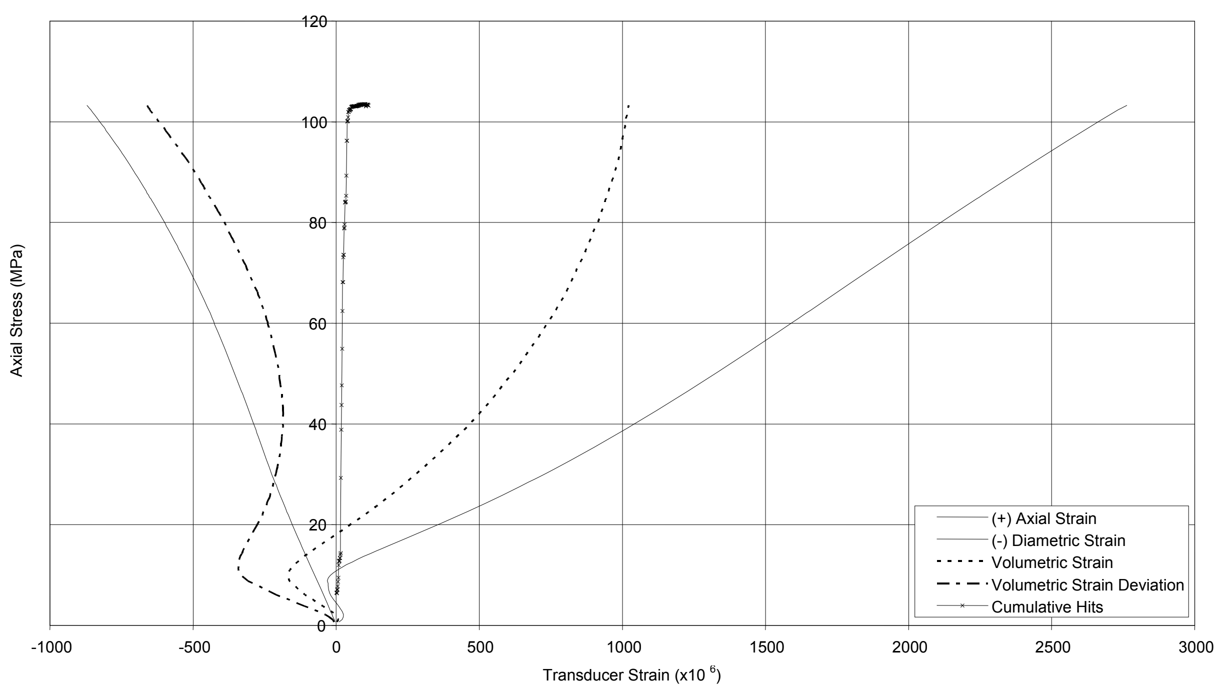


Figure B-4 UCS LSD Specimen DGR-3, 681.76 m

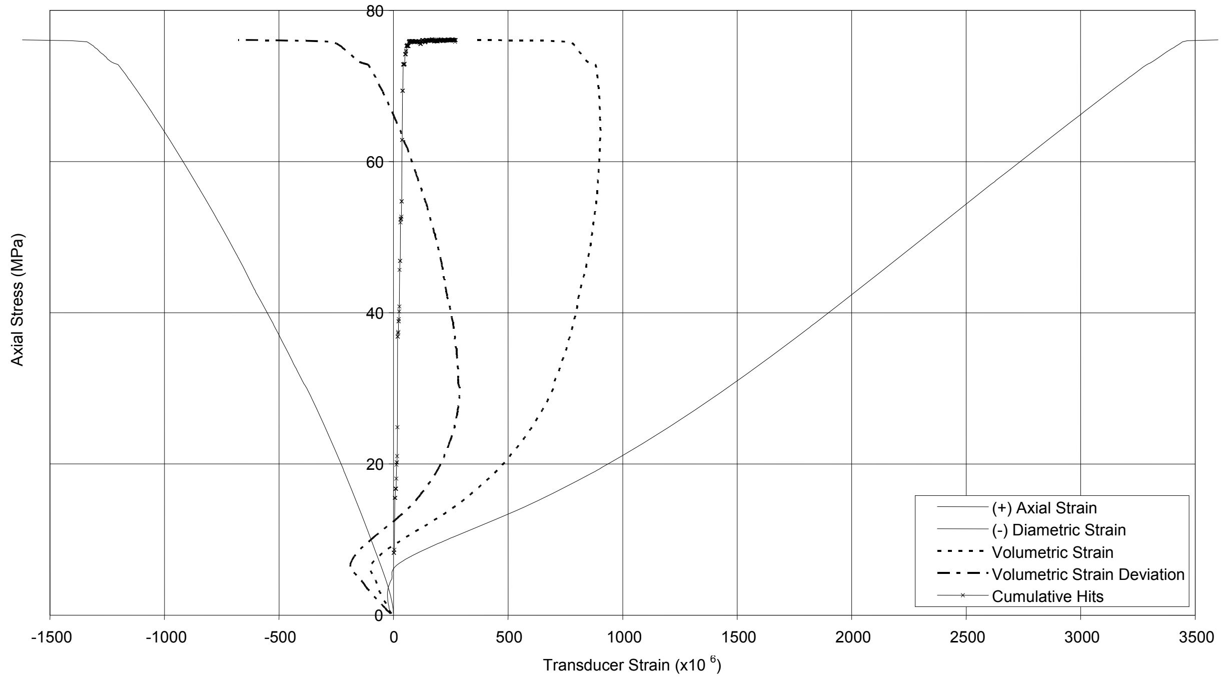


Figure B-5 UCS Specimen DGR-3, 688.13 m

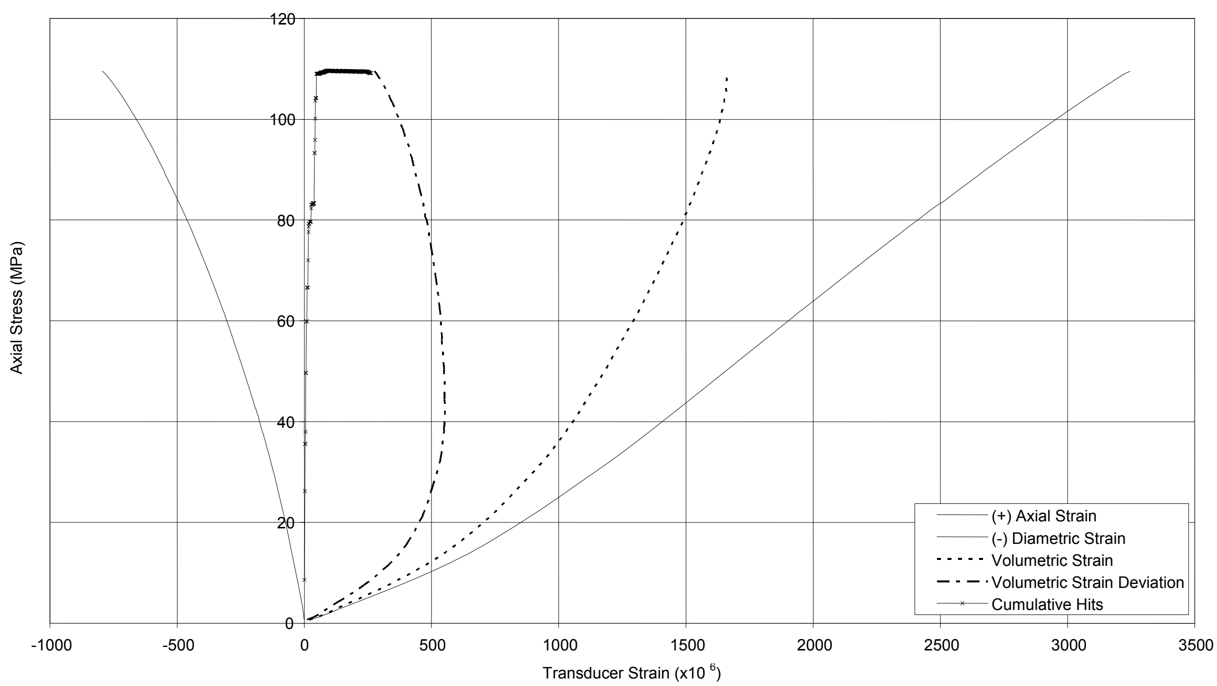


Figure B-6 UCS LSD Specimen DGR-3, 688.28 m

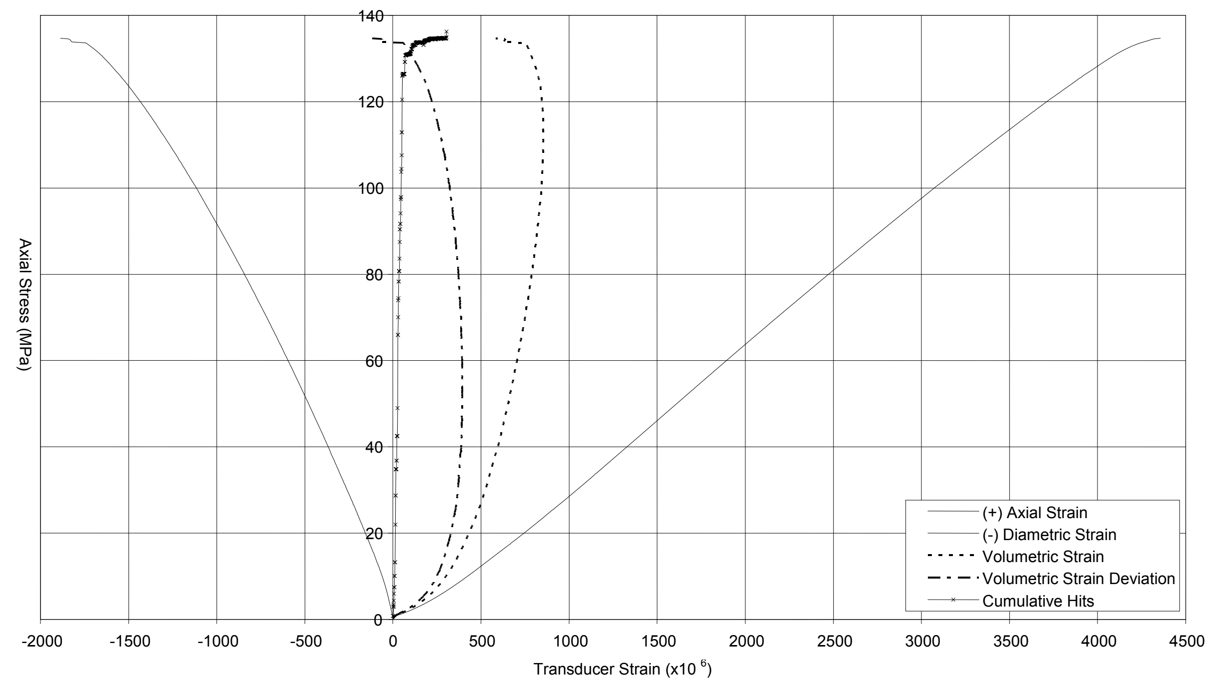


Figure B-7 UCS Specimen DGR-4, 664.46 m

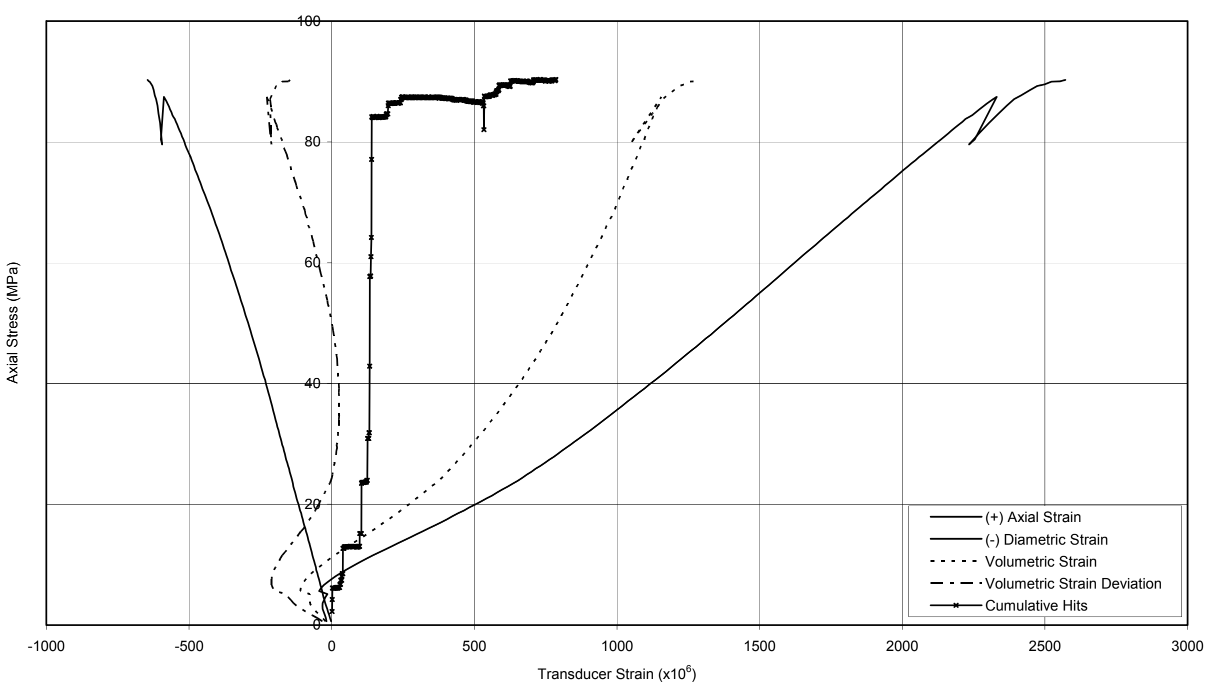


Figure B-8 UCS LSD Specimen DGR-4, 664.66 m

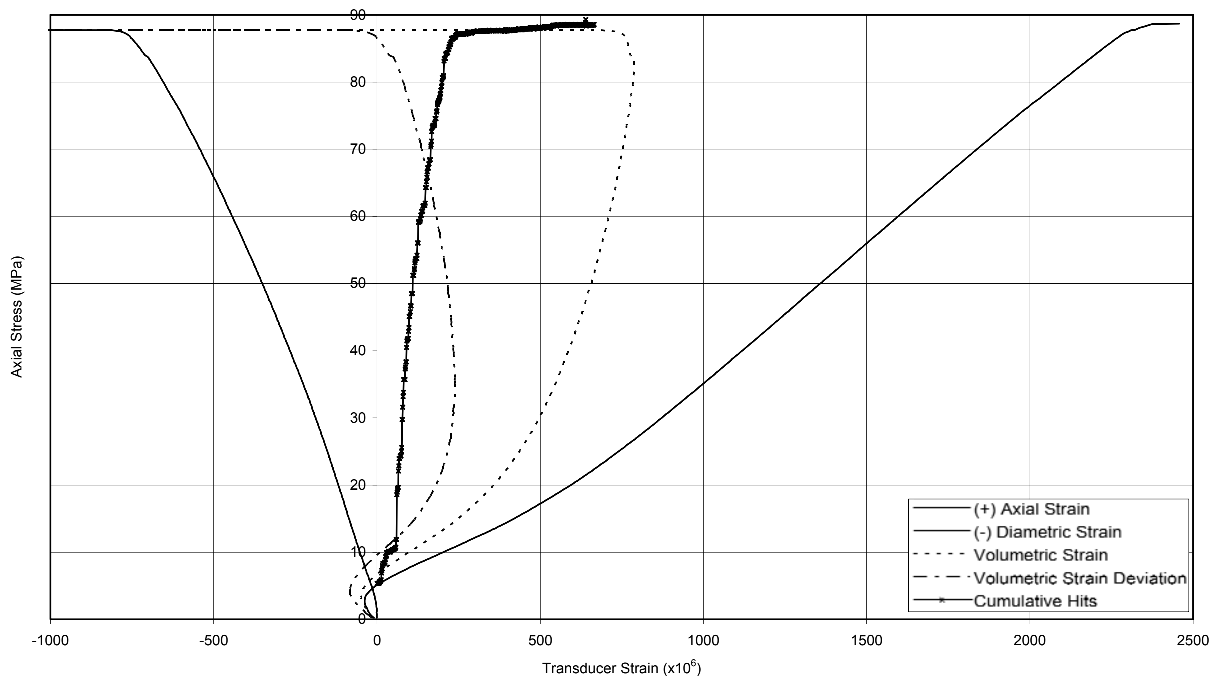


Figure B-9 UCS Specimen DGR-4, 669.90 m

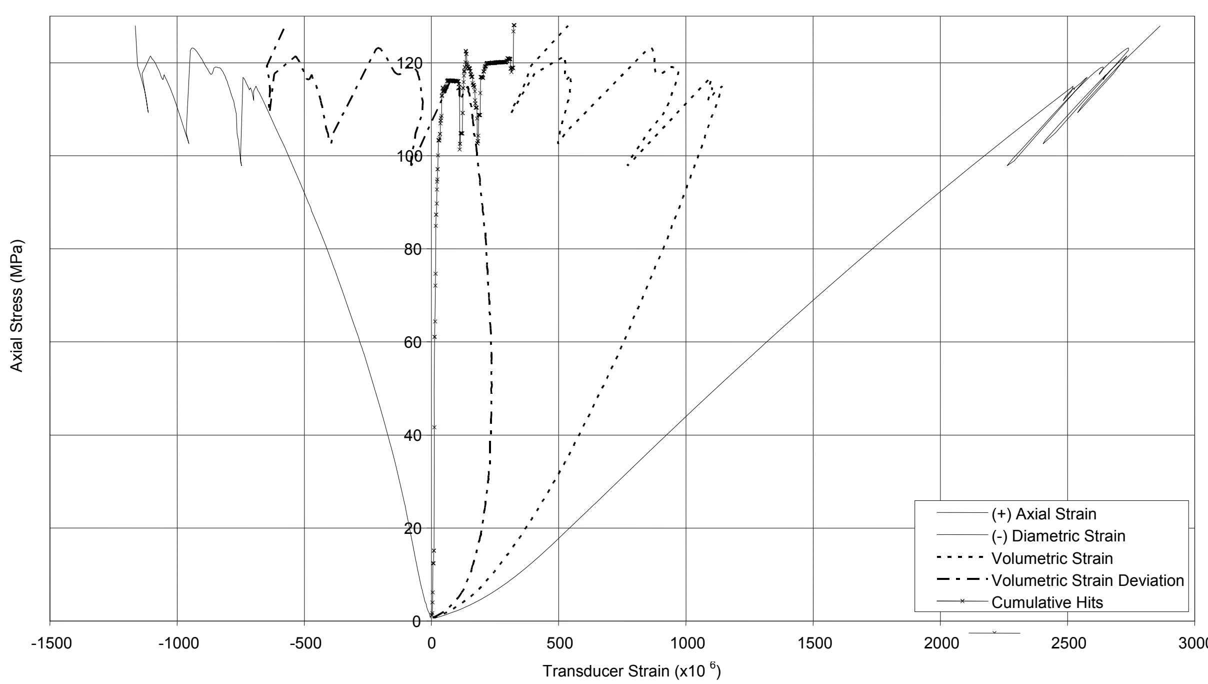


Figure B-10 UCS LSD Specimen DGR-4, 670.10 m

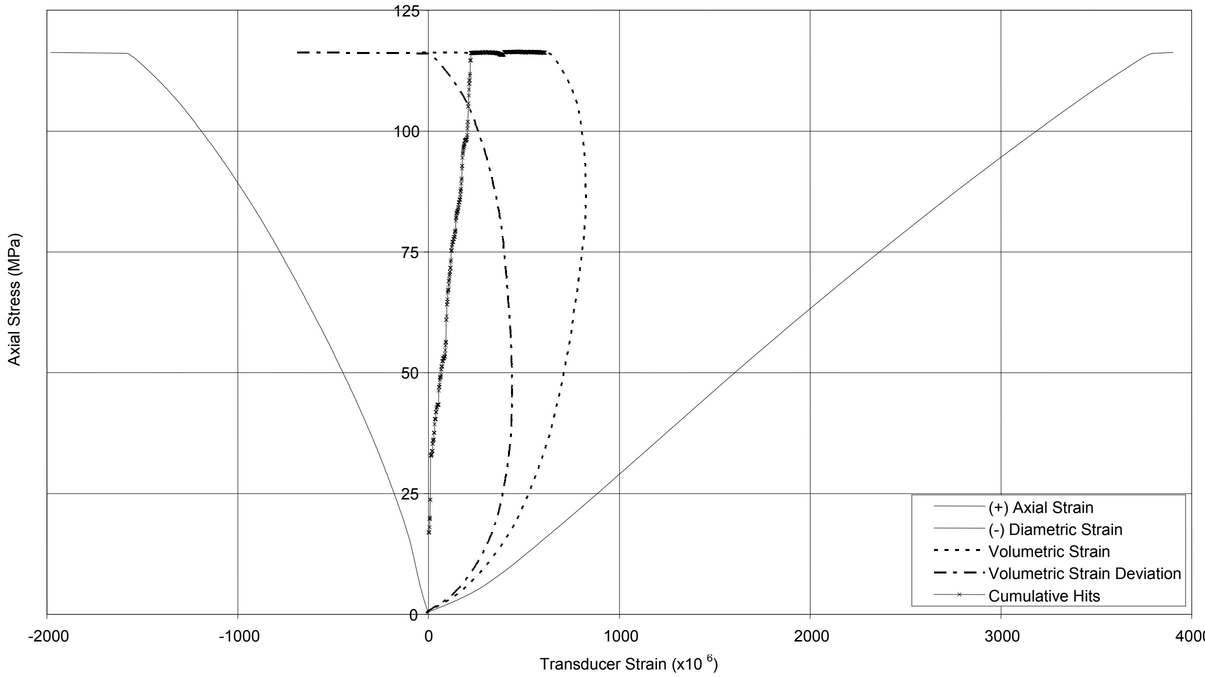


Figure B-11 UCS Specimen DGR-4, 674.16 m

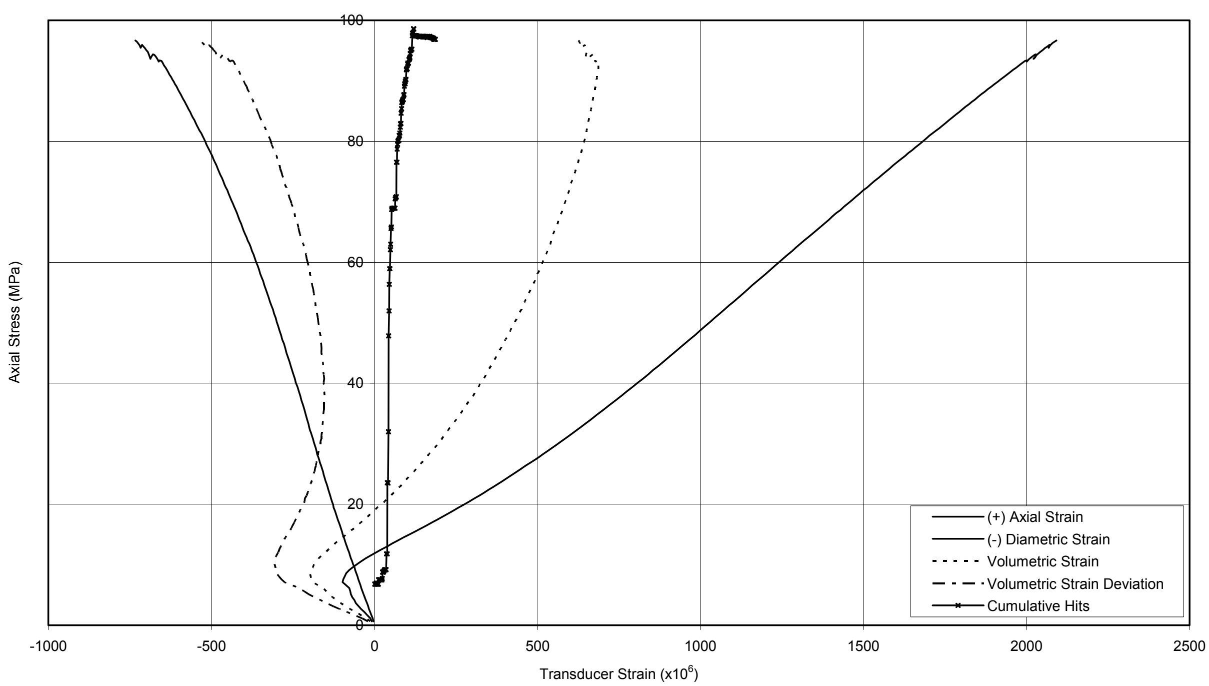


Figure B-12 UCS LSD Specimen DGR-4, 674.34 m

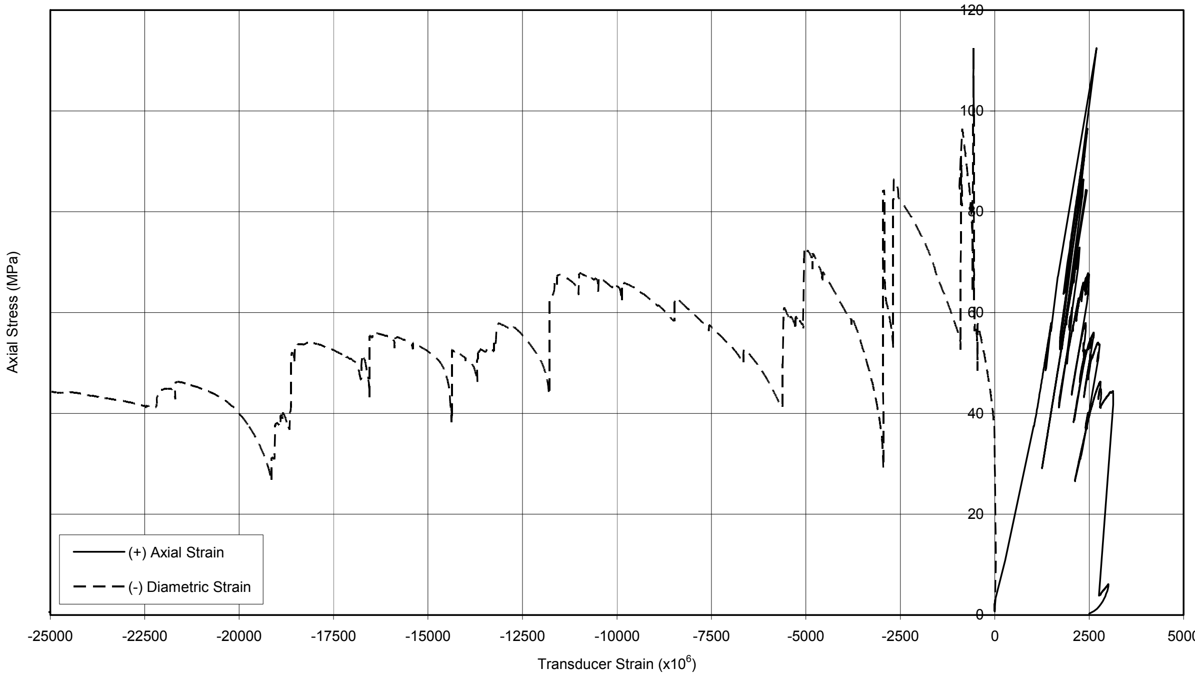


Figure B-13 UCS LSD Post-Failure Specimen DGR-3, 676.67 m

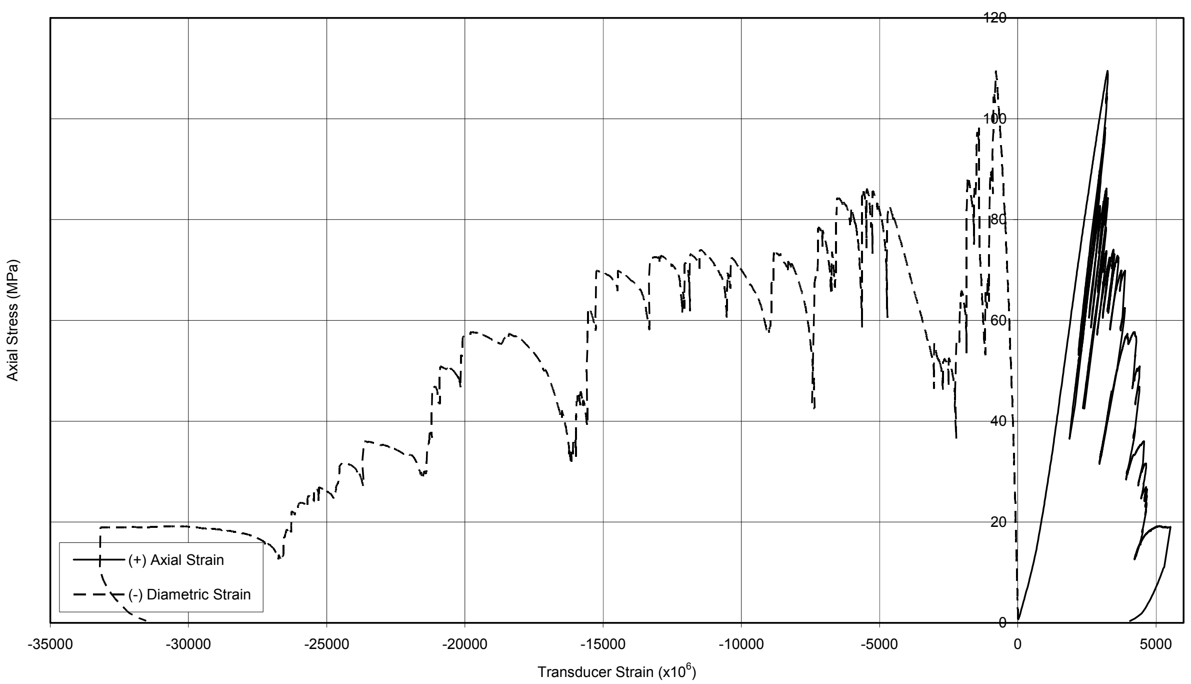


Figure B-14 UCS LSD Post-Failure Specimen DGR-3, 688.28 m

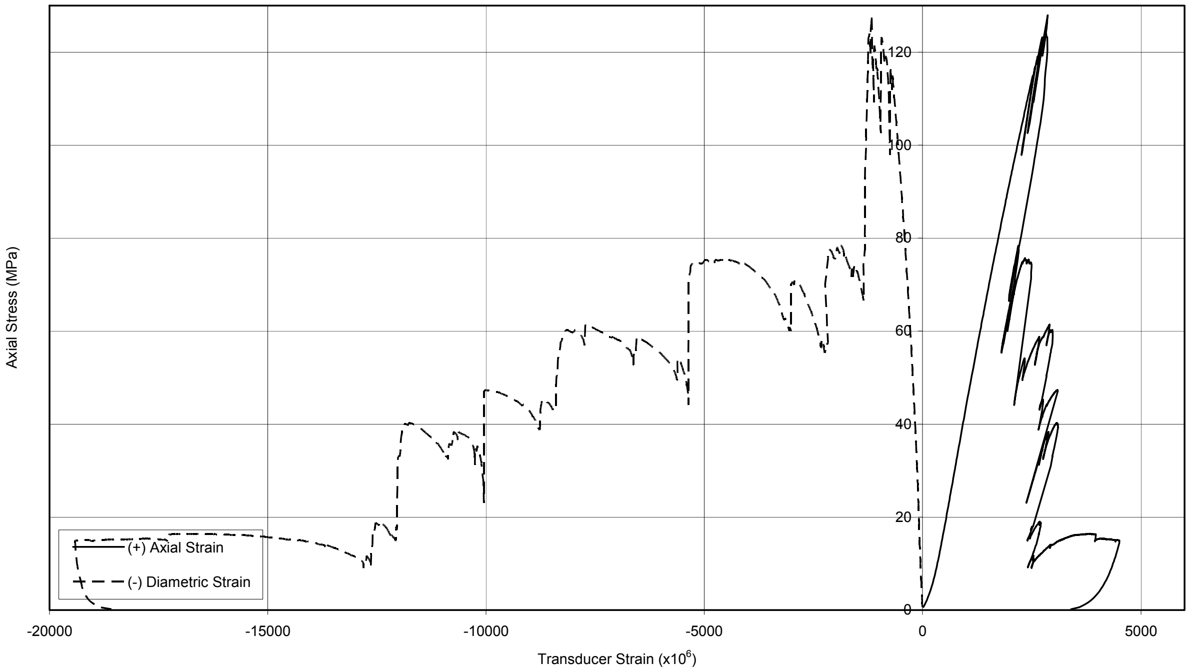


Figure B-15 UCS LSD Post-Failure Specimen DGR-4, 670.10 m

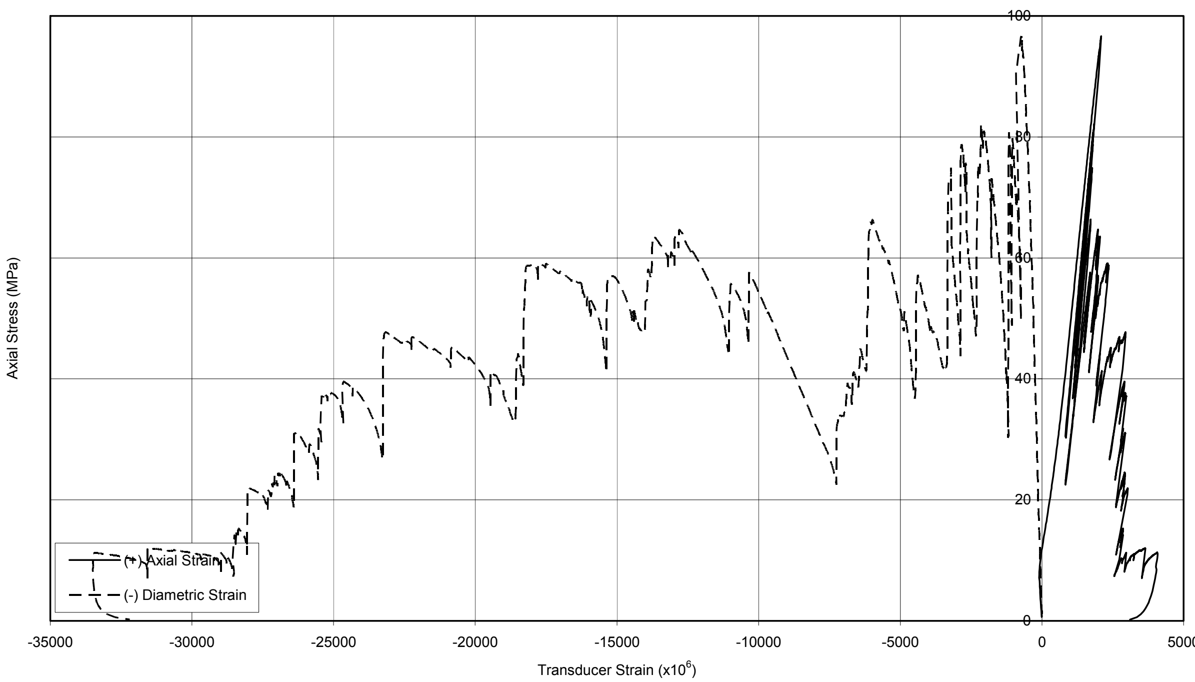


Figure B-16 UCS LSD Post-Failure Specimen DGR-4, 674.34 m

# APPENDIX C

***Failed Specimens***

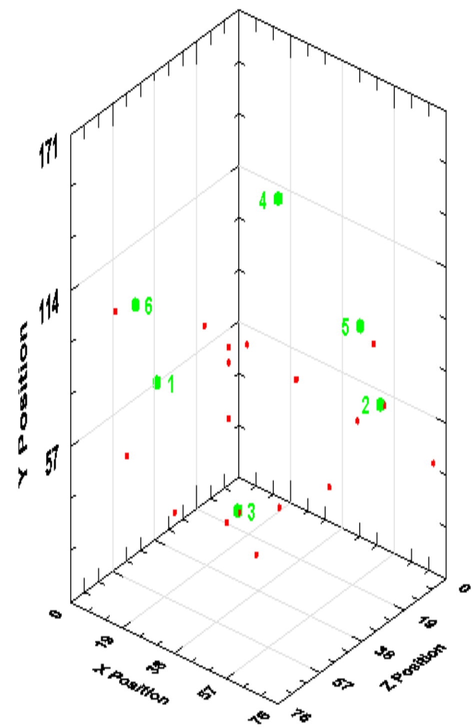


Figure C-1 Specimen DGR-3. 676.42 m

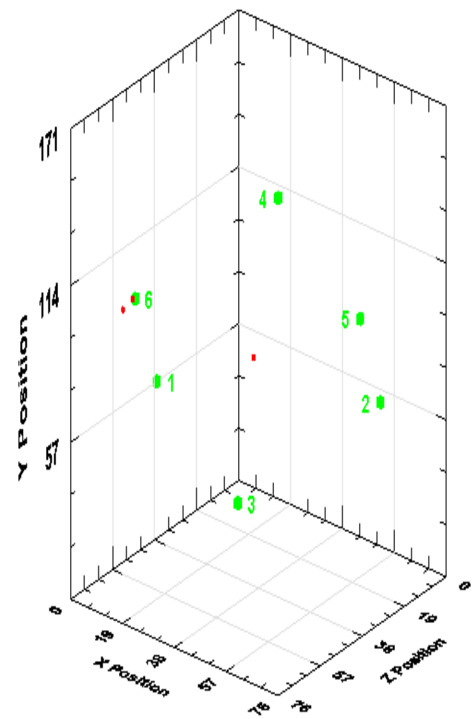


Figure C-2 Specimen DGR-3, 680.21 m

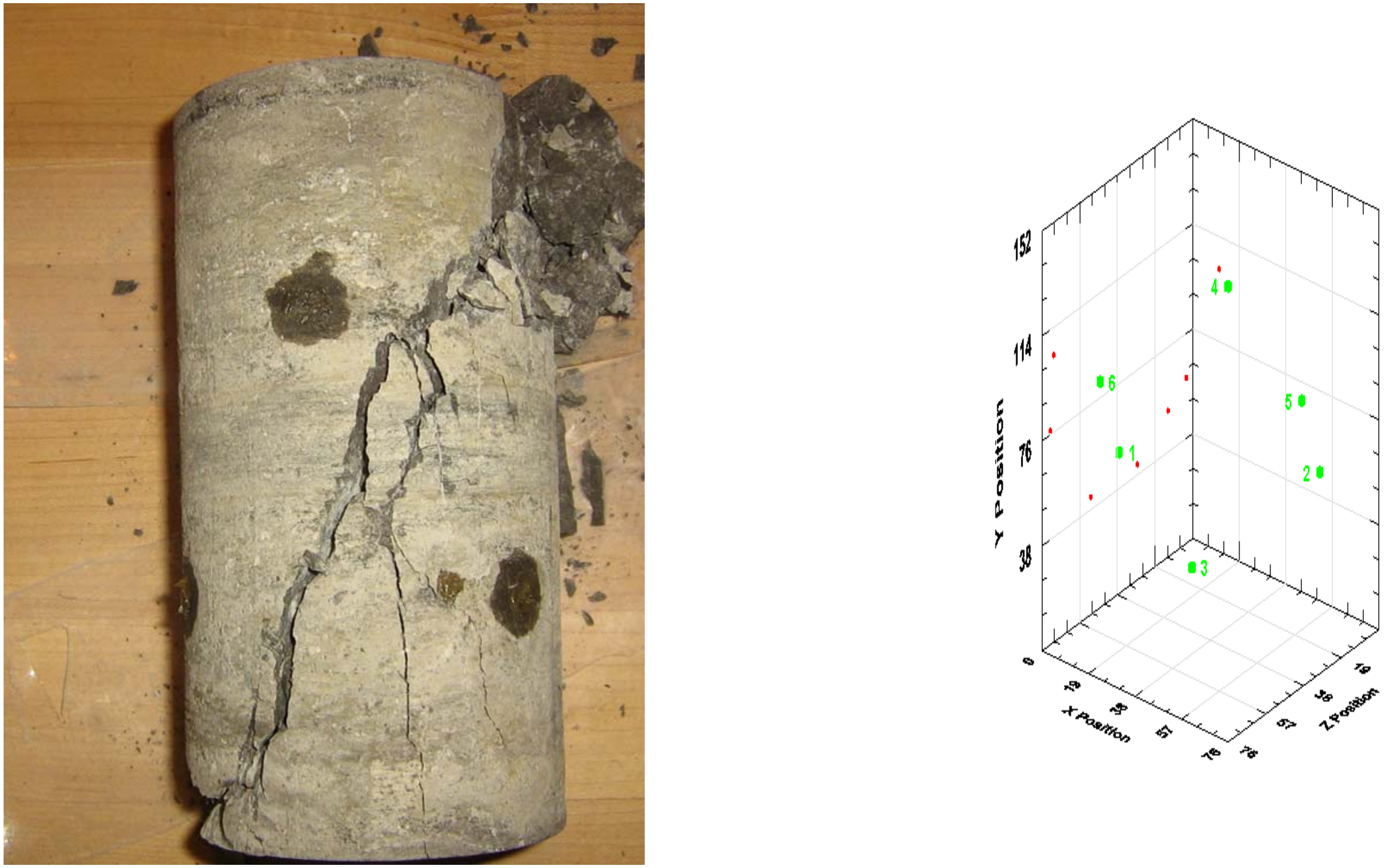


Figure C-3 Specimen DGR-3, 688.13 m

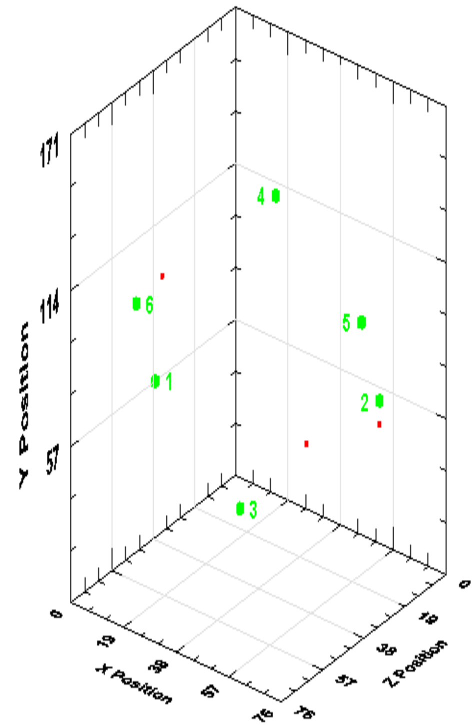


Figure C-4 Specimen DGR-4, 664.46 m

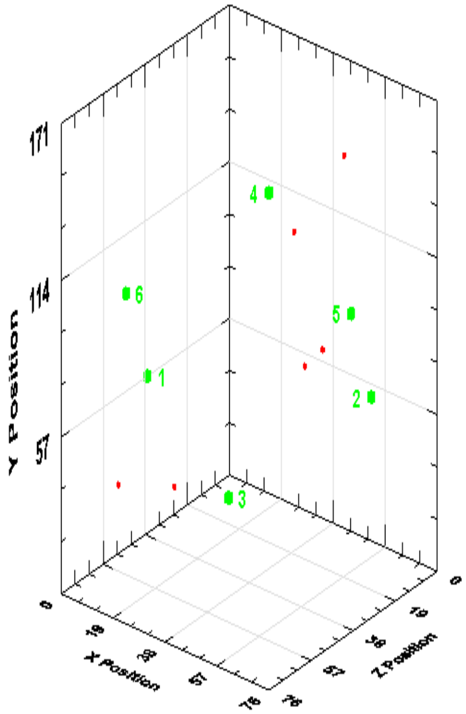


Figure C-5 Specimen DGR-4, 669.90 m

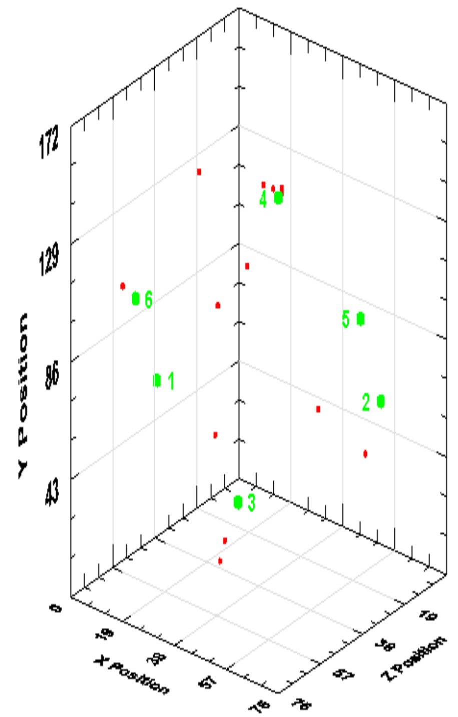


Figure C-6 Specimen DGR-4, 674.16 m


Figure C-7 Specimen DGR-3, 676.67 m

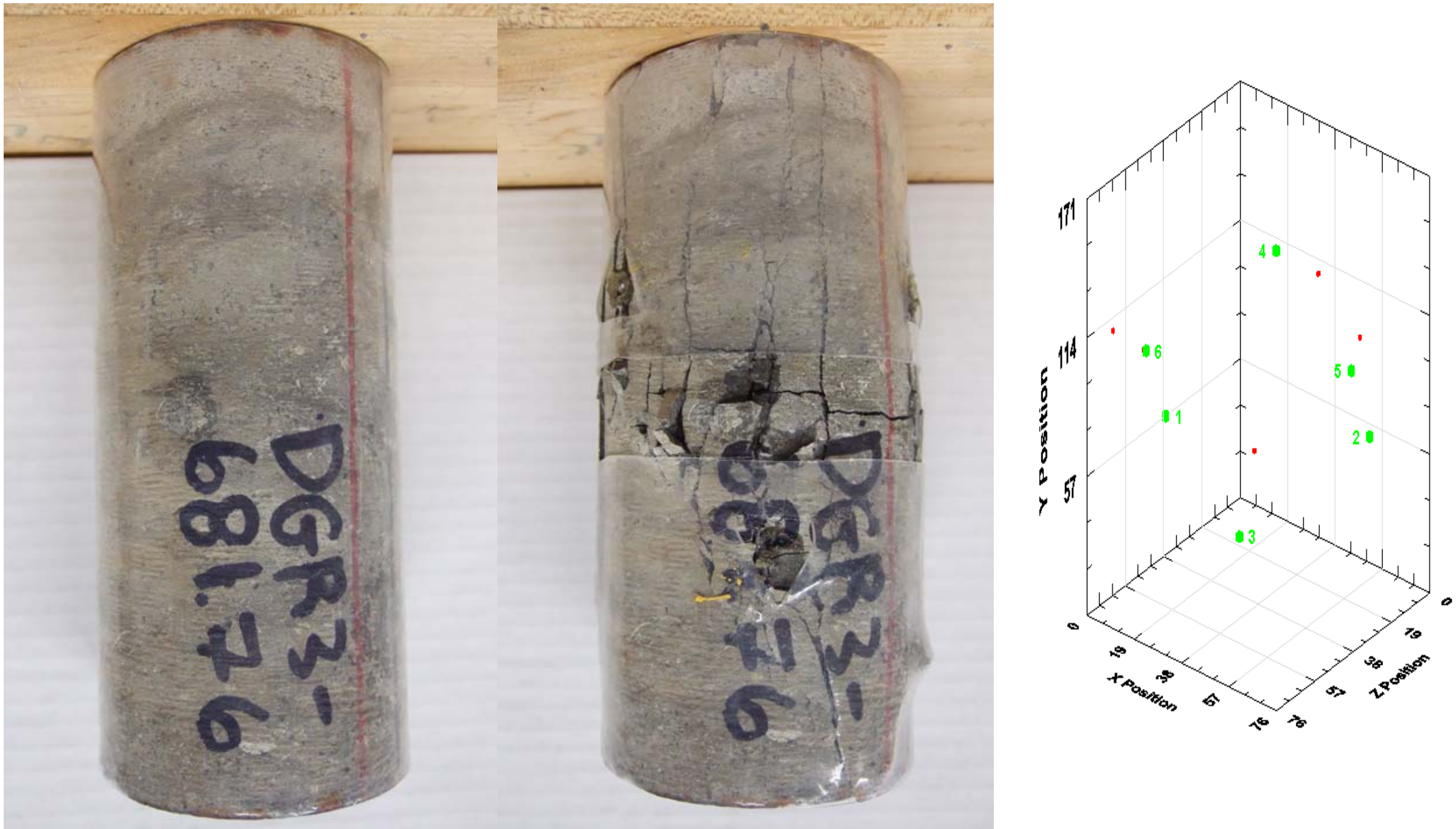


Figure C-8 Specimen DGR-3, 681.76 m

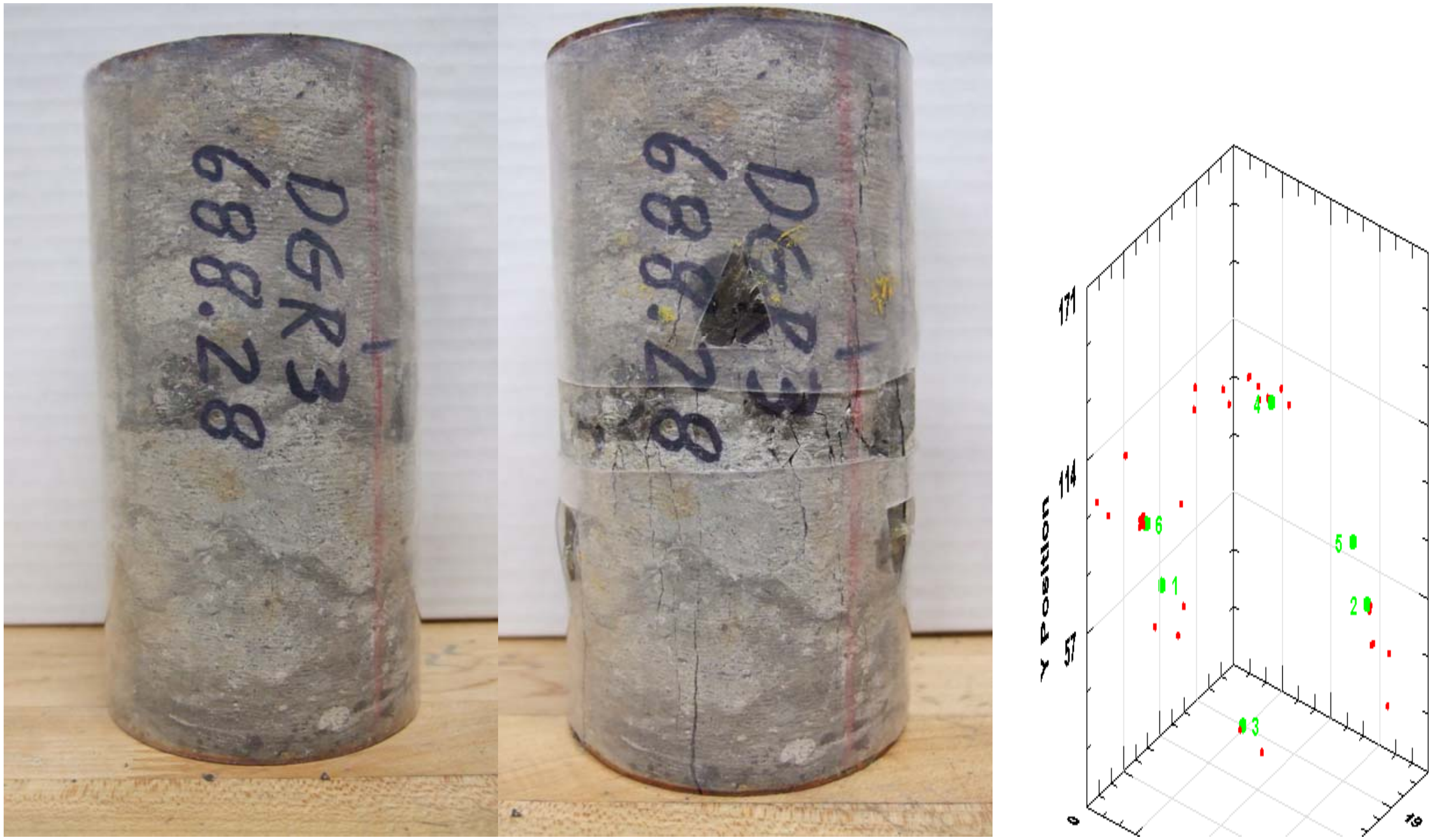


Figure C-9 Specimen DGR-3, 688.28 m


Figure C-10 Specimen DGR-4, 664.66 m


Figure C-11 Specimen DGR-4, 670.10 m


Figure C-12 Specimen DGR-4, 674.34 m

## APPENDIX D

***Plots of Axial and Diametric Displacement vs. Time***

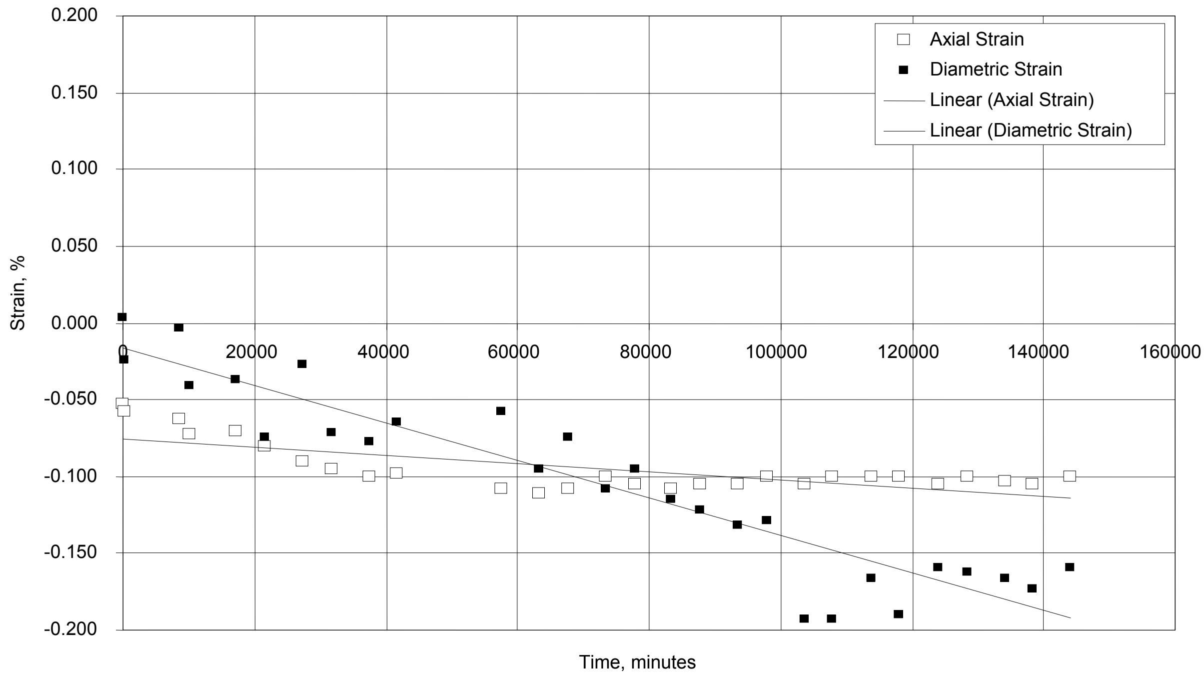


Figure D-1 Specimen DGR-4, 676.67 m

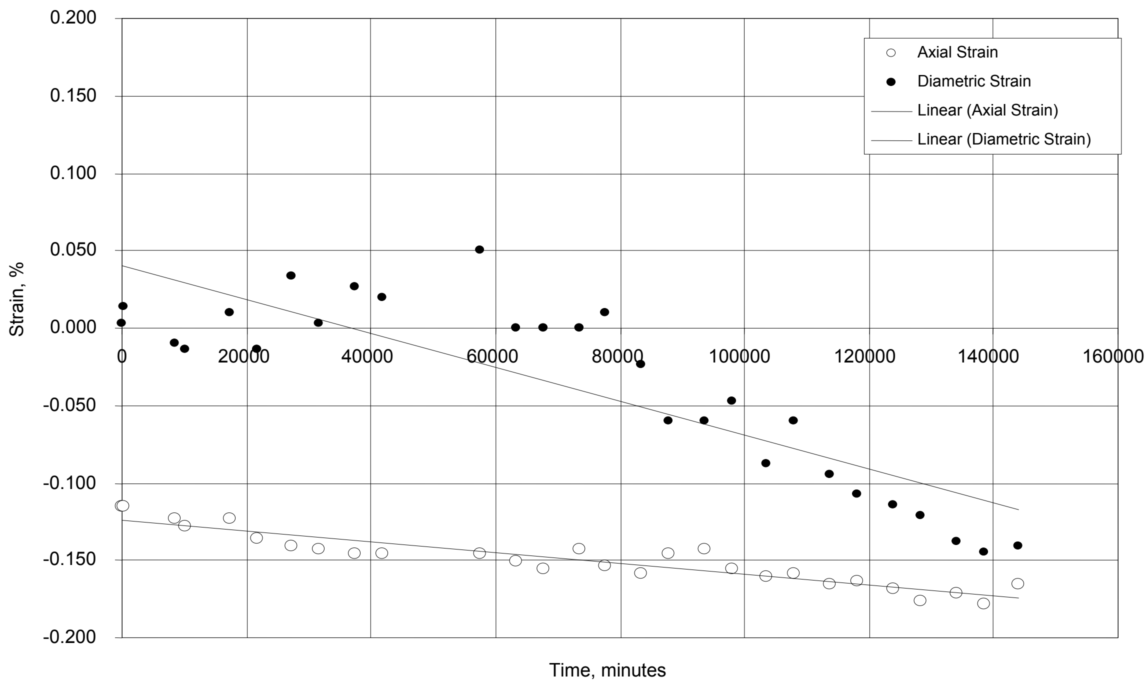


Figure D-2 Specimen DGR-4, 681.76 m

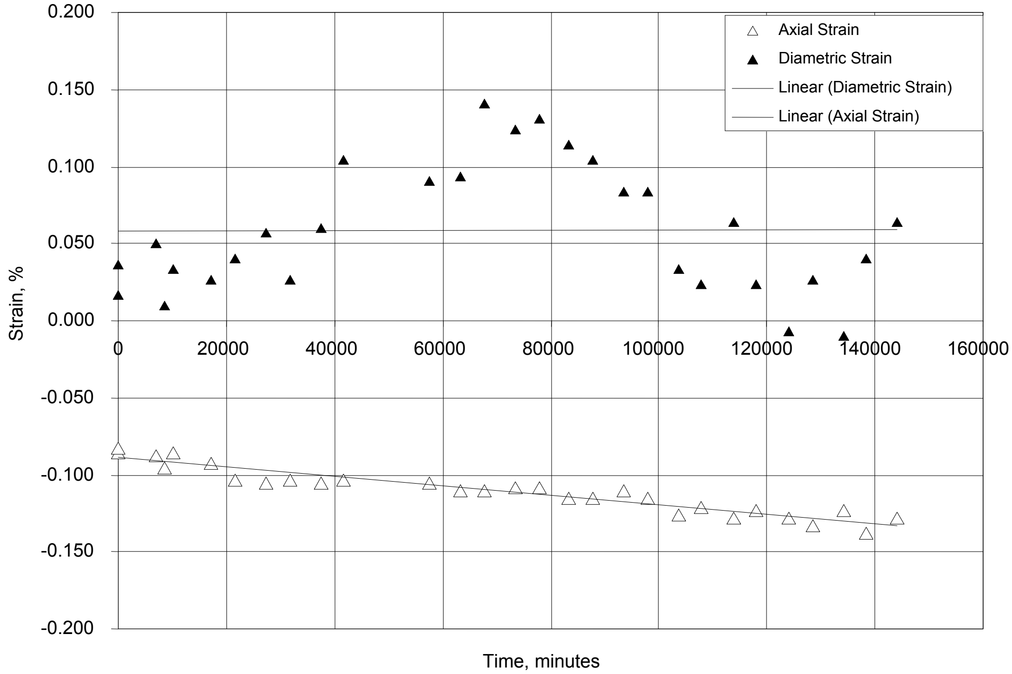


Figure D-3 Specimen DGR-4, 688.28 m

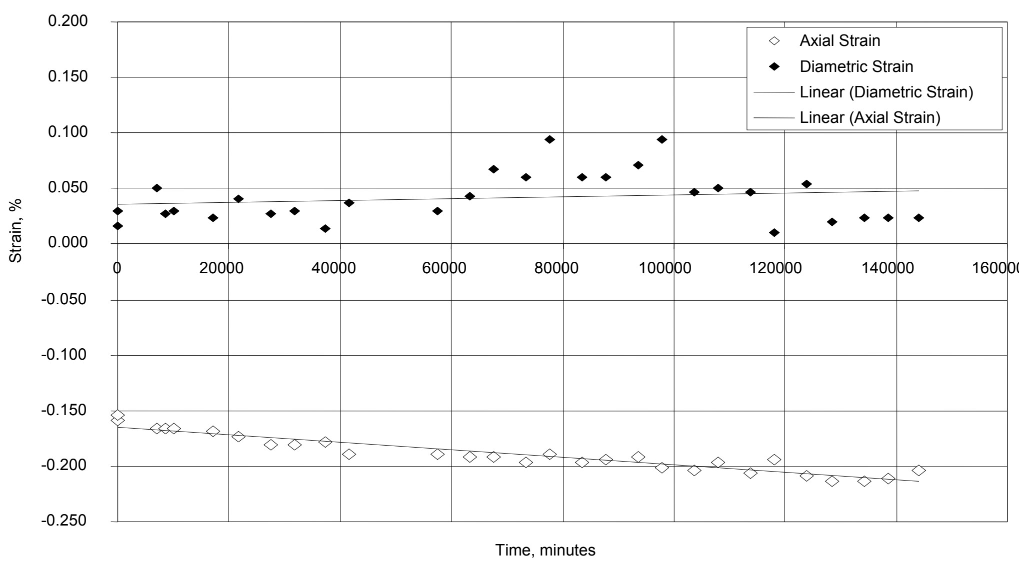


Figure D-4 Specimen DGR-4, 664.66

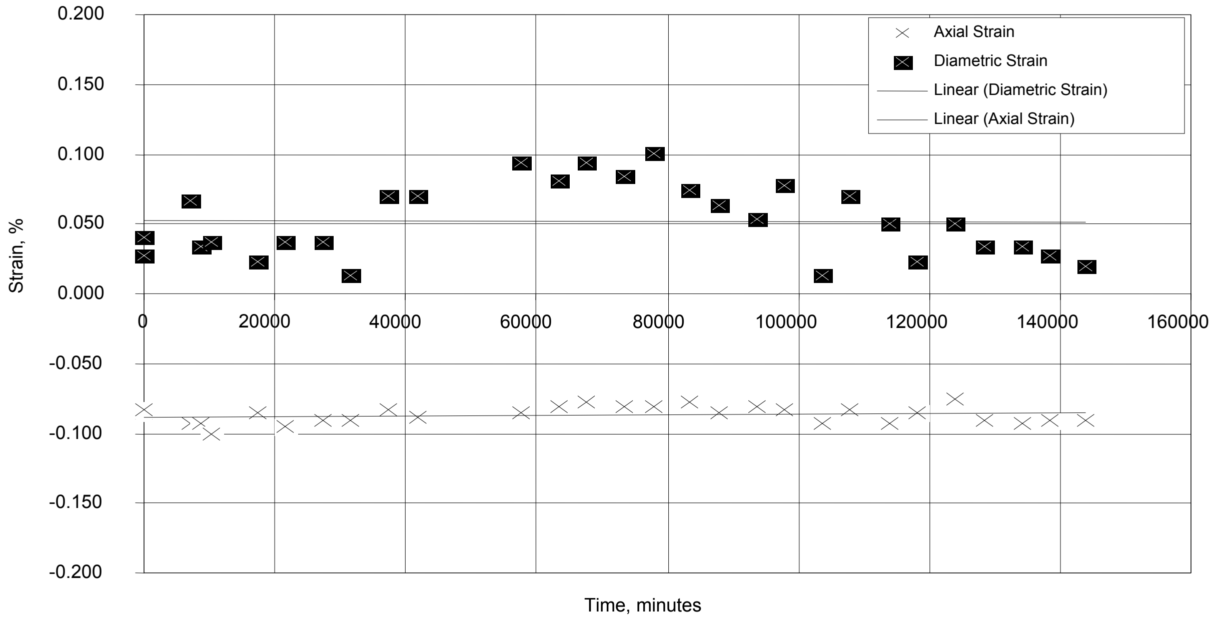


Figure D-5 Specimen DGR-4, 670.10 m

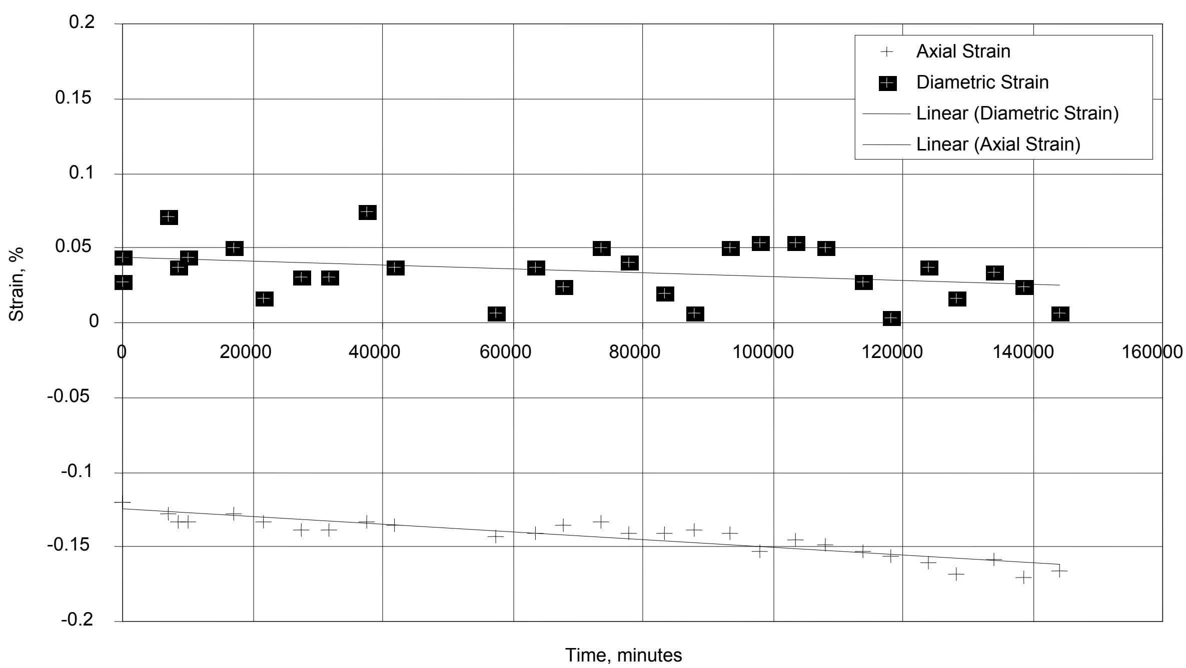


Figure D-6 Specimen DGR-4, 674.34 m

# APPENDIX E

***Plots of AE Cumulative Hits vs. Time***

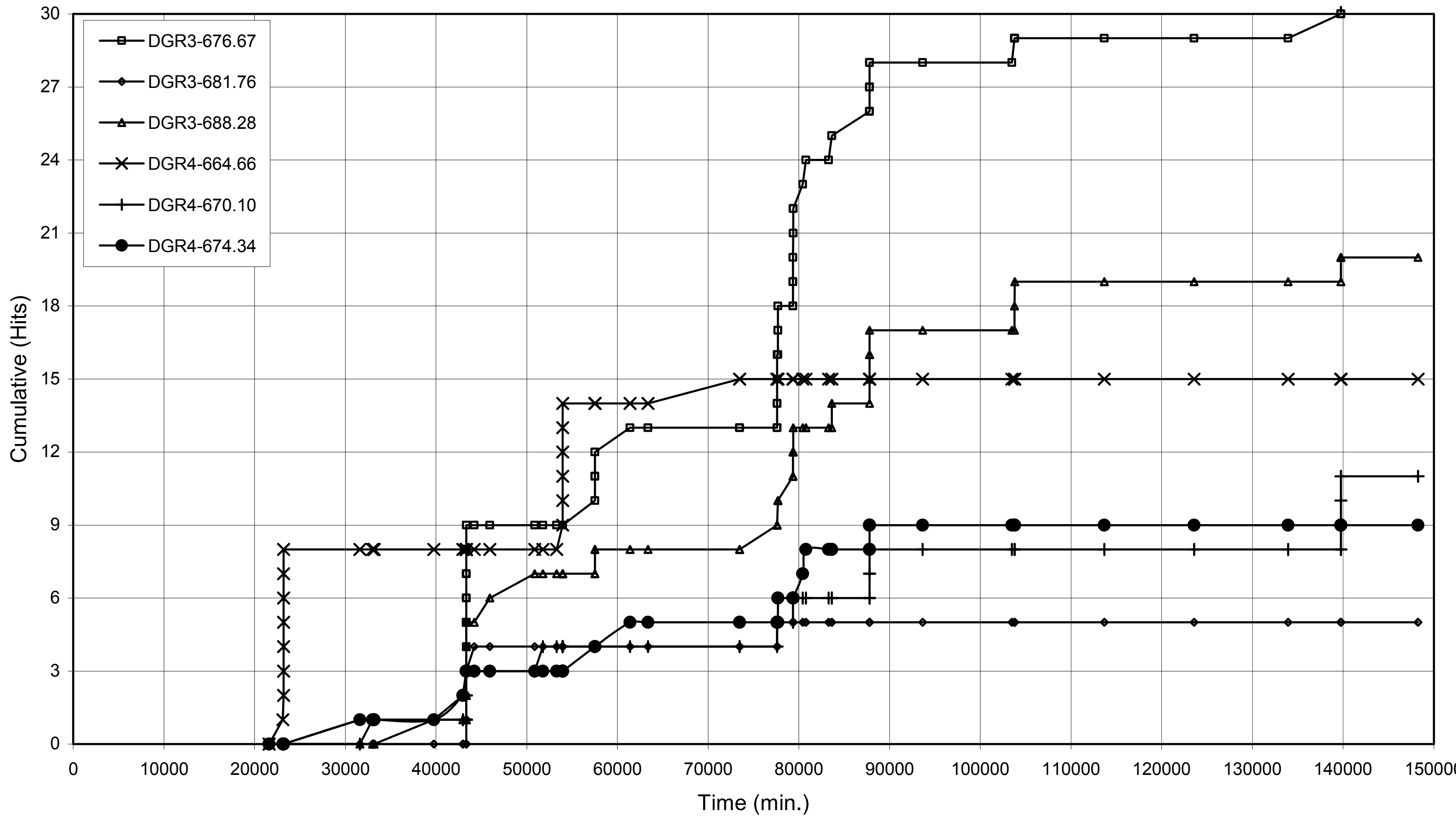


Figure E-1 Cumulative AE Hits vs. Time